A NOVEL CONTROL APPROACH FOR SWITCHED RELUCTANCE MOTORS BASED ON FUZZY LOGIC AND PARTICLE SWARM OPTIMIZATION TECHNIQUES

Thi Mai Phuong DAO[1], Yao Nan WANG[2], Ngoc Khoat NGUYEN[3]

A novel control approach to design efficient speed controllers for Switched Reluctance Motor (SRM) drives based on fuzzy logic (FL) and Particle Swarm Optimization (PSO) techniques is investigated in this study. The PSO mechanism with the simple implementation and high efficiency is adopted to optimize five parameters, including three scaling factors of a PI-like FL architecture and two switching factors of an asymmetrical DC-DC voltage converter. Resulting from this optimization process, an adaptive FL control strategy for the SRM drive can be fulfilled to obtain the highly promising control performances. Various numerical simulations are also performed for the demonstration purpose.

Keywords: Switched Reluctance Motor (SRM) drive system, Particle Swarm Optimization (PSO) algorithm, PI-type FL controller, Switching Angles.

1. Introduction

It is the fact that Switched Reluctance Motors (SRMs) have been applied efficiently in plenty of practical drive systems requiring the variable speed due to their outstanding advantages [1, 2]. Various applications of the SRM drives have been found in [2]. Together with the typical prototypes, such as 6/4 (three phases) and 8/6 (four phases), the novel kinds of the SRMs have been continuously investigating in order to seek the perfect structures of electrical machines for the future of effective drive systems [3, 4].

Even though there exist a lot of increasing applications, the SRMs are still being studied in dealing with their inherent disadvantages, e.g., the nonlinearity, the torque ripple and the difficult control of electronic power converters, which are used to feed the energy to the machines [5-7]. It is found that the efficient control strategies need to be investigated to obtain the permissible control

[1] PhD candidate, College of Electrical and Information Engineering, Hunan University, Changsha, Hunan 410082, China; Faculty of Electrical Engineering Technology, Hanoi University of Industry, Hanoi, Vietnam, email: daophuong@haui.edu.vn

[2] Prof., College of Electrical and Information Engineering, Hunan University, Changsha, Hunan 410082, China

[3] PhD, Researcher, Faculty of Automation Technology, Electric Power University, Hanoi, Vietnam

performances, such as the good stability, high efficiency and the optimal dynamic responses of the phase current, electromagnetic torque as well as the angular speed. In general, control strategies, which mainly focus on designing speed and current controllers, have applied both the conventional and modern regulators. The conventional controllers (i.e., PI and PID regulators) have been considered initially due to their simplicity of the design and operation [2]. Nevertheless, the poor control characteristics obtained, such as the high overshoot, the long rise time and settling time as well as the large reduction of speed due to load torque, have restricted the widespread use of such controllers. Hence, these regulators should be replaced with the improved controllers using the modern techniques, e.g., fuzzy logic (FL), in order to attain the better control properties. Based on the FL technique, the PI-type FL controllers (FLCs) have been applied widely and efficiently in many control systems [8-10], especially in the SRM drives.

In the context of applying a PI-type FLC to the speed regulation of an SRM system, scaling factors, which affect significantly the control performances of the drive system, must be tuned properly in order to obtain the desired quality and efficiency. Many reports have been published to deal with this problem [7, 11]. However, the SRM drive system, which is supplied by an electronic power converter (e.g., an asymmetrical DC-DC converter), is usually subject to the switching states of the semiconductor devices [2]. This leads to the difficulty of the control strategies to achieve entirely the permissible characteristics. Basically, an optimal control strategy applying the FLCs has to make sure that not only the parameters of such FLCs but also the switching angles of the converter should be optimized in an effective manner.

Particle Swarm Optimization (PSO) mechanism, which is one of the most effective biological-inspired optimization techniques [12], will be applied in this study as an effective candidate to solve the above problem. With an online implementation through several appropriate steps, the PSO mechanism can optimize effectively three scaling factors of the PI-type FLC (two inputs and one output) as well as two switching angles (turn-ON and turn-OFF angles) of the voltage-source DC-DC converter. Resulting from such an optimization process, five parameters obtained can be used to design an adaptive control strategy based on the PI-type FL architecture for a particular SRM drive. In this paper, a three-phase SRM model (6/4-type machine) is selected for the simulation aim to validate the feasibility of the proposed control scheme. Based on the PSO algorithm, two simulation cases, including for tuning only the scaling factors of the FL architecture and for all the FLC and switching angles, with various cases of load torques will be performed. Applying both the PSO-PI-type FLC and the conventional PI regulator to design the speed controllers, simulation results obtained are quite able to be used to demonstrate the feasibility and efficiency of the adaptive control strategy presented in this work.

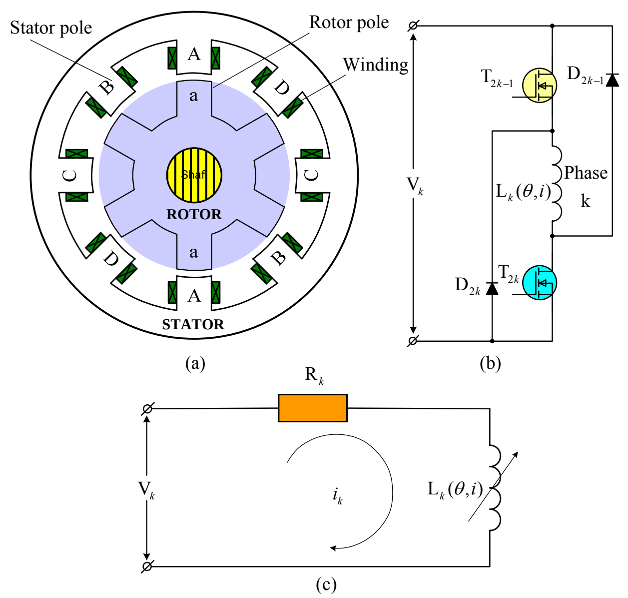

Fig. 1. A typical configuration of 8/6-type SRM
(a) Cross-section; (b) Phase *k*-th feeding; (c) An equivalent circuit for the *k*-th phase

2. Mathematical Model of an SRM

In terms of the physical structure, an SRM is considered to be a doubly salient pole and singly excited machine. The SRM is typically fed by a DC power source, such as a voltage- or current-type DC source feeding. Thus, a unipolar electric power inverter, e.g., DC-DC or AC-DC converter, can be used. A DC-DC converter is typically an electronic circuit which can be used to convert a DC power supply to another with different level of voltage. It means that it is able to be adopted to change a DC power supply in terms of the voltage value for a particular regulating purpose. Fig. 1(a) shows the cross-section of a typical family of the SRMs, i.e., 8/6-type SRM. Here, the stator has 8 poles (4 pole-pairs wound by serially concentrated windings) corresponding to 4 phases: A, B, C and D. Meanwhile, the rotor, which is composed of neither windings nor magnets, has 6 poles (see Fig. 1(a)). The configuration of the *k*-th phase winding connected to the corresponding phase of an asymmetrical DC-DC inverter is described in Fig. 1(b). Despite the simplicity of the construction, it is highly difficult to design an exactly mathematical model of an SRM due to its nonlinear characteristics. All of its characteristics including flux linkage, inductance and torque are nonlinearly dependent upon the variation of not only the phase current but also the rotor position during the operation of the machine [2]. In order to simplify the modeling process, each phase of the SRM can be replaced with an equivalent circuit, including a winding resistance in series with an inductance as shown in Fig. 1(c). Such inductance will be considered as a function of both the phase current and the rotor position when computing the flux linkage of the *k*-th phase as expressed below:

$$\Psi_k(i_k,\theta)=\sum_{l=1}^{n}L_{kl}(i_k,\theta).i_k(t) \qquad k=1,2,\ldots\mathrm{n} \tag{1}$$

where $\Psi_k(i_k,\theta), i_k(t)$ and θ denote the flux linkage, phase current and rotor position of the *k*-th phase, respectively. Meanwhile, the value of $L_{kl}(i_k, \theta)$, which is a mutual inductance between the *k*-th phase and the *l*-th phase, can be neglected since it would be much smaller than the corresponding bulk inductance [3-4].

The instantaneous *k*-th phase voltage of an SRM can be calculated as:

$$V_k(t)=R_k i_k(t)+\frac{d\Psi_k(i_k,\theta)}{dt} \tag{2}$$

where R_k is the winding resistance of the *k*-th phase. From (1) and (2), using the derivative calculus of multivariable functions, one can be obtained below:

$$V_k(t)=R_k i_k(t)+\sum_{l=1}^{n}\left[\left(L_{kl}(i_k,\theta)+i_k(t).\frac{\partial L_{kl}}{\partial i_k}\right)\frac{di_k}{dt}+i_k(t).\frac{\partial L_{kl}}{\partial\theta}.\omega\right] \tag{3}$$

where, $\omega=d\theta/dt$ is the angular speed of the SRM. Neglecting the mutual inductances, the instantaneous *k*-th phase voltage can be rewritten as follows:

$$V_k(t)=R_k i_k(t)+\left(L_k(i_k,\theta)+i_k(t).\frac{\partial L_k}{\partial i_k}\right)\frac{di_k}{dt}+i_k(t).\frac{\partial L_k}{\partial\theta}.\omega \tag{4}$$

where $L_k(i_k, \theta)$ denotes the *k*-th phase bulk inductance. The mechanical equation describing the motion of an SRM is given as:

$$J.\frac{d\omega}{dt}=T-T_L-f.\omega \tag{5}$$

where J, f, T_L and T are the total inertia, the friction coefficient, the load torque and the total output torque, respectively. The total output torque is calculated as:

$$T=\sum_{k=1}^{n}T_k(i_k,\theta) \tag{6}$$

where $T_k(i_k, \theta)$ denotes the *k*-th phase torque computed depending on the derivative of the co-energy. The mathematical model represented in (2) and (5) is able to be adopted for designing control strategies of an SRM. A speed control methodology for the SRM drive system will be presented in the following section.

3. Basic FL-Based Speed Control Architecture for the SRM Drive

The conventional PI-based FL speed controller for an SRM drive system is normally described in Fig. 2. In this control strategy, two inputs $\left(e_N[j], \Delta e_N[j]\right)$

and one output $(\Delta u_N[j])$ are used for the FL inference system. Such two inputs are proportional directly with the error of the angular speed $e[j]$ and its change $\Delta e[j]$ through two gains of K_1 and K_2, respectively. Meanwhile, the output is employed to generate the control signal $u[j]$, which is fed directly to the SRM drive model.

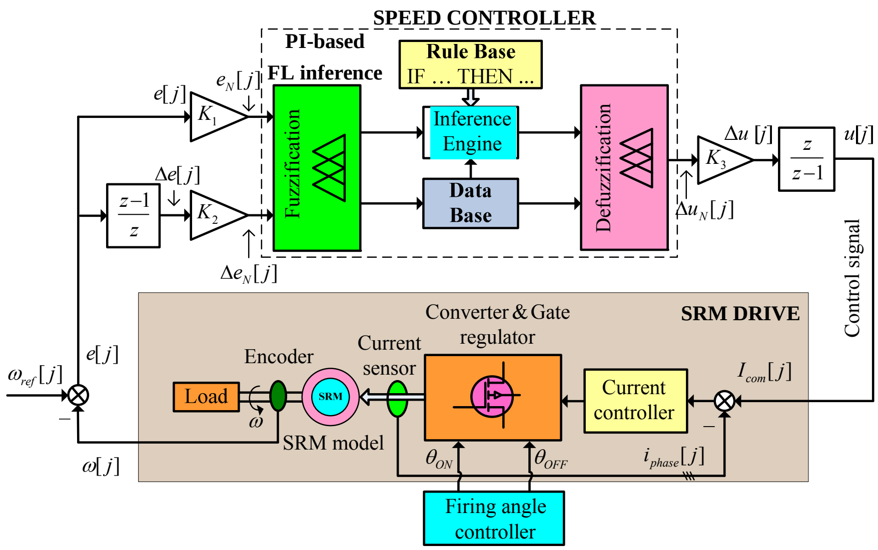

Fig. 2. A fundamental control architecture based on PI-like FL speed controller

As shown in Fig. 2, a FLC model includes three basic blocks: the knowledge base which contains rule base, data base and the inference mechanism, the fuzzification and the defuzzification interface [12]. Each block performs a particular functionality for the implementation of this FL architecture. In general, the first block (fuzzification) is used to convert the inputs into fuzzy sets. Subsequently, the second mechanism will process the fuzzy sets which are obtained in the previous phase. A rule base in this phase is a set of linguistic "IF – THEN" constructions that have a general form "IF A THEN B", where A and B are propositions containing linguistic variables. Normally, A is called the premise and B is the consequence of the rule. In addition to the rule base, a fuzzy inference engine (reasoning) is the actual process of mapping from a given input to an output using fuzzy logic. The design of rule base as well as the implementation of the inference engine inside the second mechanism are based on a data base. This is built by experts depending upon their understanding of the control systems which are being taken into account. After this reasoning phase, the defuzzification is finally employed to convert the results achieved above into the corresponding outputs of the FL architecture. It is the fact that all of the inputs and output of an FL inference system should be considered to be crisp signals when they are processed. The principle of a PI-type FL inference system relies upon the crisp relationship between its inputs and output, which is similar to a classical PI regulator. The classical PI regulator is expressed as follows:

$$u(t) = K_p.e(t) + K_I.\int_0^t e(\tau)d\tau \tag{7}$$

where K_P, K_I, $e(t)$ and $u(t)$ denote the proportional gain, the integral constant, the input error signal and the output of the regulator, respectively. Using the derivation and converting the result into the discrete form, (7) can be rewritten as:

$$\Delta u[j] = K_P.\Delta e[j] + K_I.e[j] \tag{8}$$

It is clear from Fig. 2 that the relationship between two inputs and one output of the FL inference can be written as follows:

$$\Delta u[j] = K_3.\left(\mu_1.K_1.e[j] + \mu_2.K_2.\Delta e[j]\right) \tag{9}$$

where K_i (i = 1, 2, 3) and μ_k (k = 1, 2) are scaling factors and internal gains of the FL reasoning system. Hence, from (9), one can be drawn below:

$$\Delta u[j] = K_P^{FLC}.\Delta e[j] + K_I^{FLC}.e[j] \tag{10}$$

Two factors mentioned in (10), $K_P^{FLC} = \mu_2.K_2K_3$ and $K_I^{FLC} = \mu_1.K_1K_3$, can be considered to be the proportional and integral gains associated with those of the classical PI regulator (see (7)). In the following section, both of these factors will be determined efficiently by using the PSO algorithm.

4. Adaptive PSO-PI-type FL-Based Speed Control Strategy

In order to design an adaptive speed controller for the SRM drive using the FL technique, an optimization method, named Particle Swarm Optimization (PSO), will be adopted. It is well known that the PSO would be one of the most effective optimization algorithms applied in a large number of control problems. The executed mechanism of the PSO was reported in [12]. The proposed control scheme applying the PSO mechanism is illustrated in Fig. 3. It is clear this model has been built by modifying Fig. 2. As shown, the block "PSO algorithm operator" is to perform the PSO mechanism, which has been presented in [12]. The other blocks are described in detail below.

For a PI-type FL controller, it is highly necessary to determine the optimal values of K_P^{FLC} and K_I^{FLC} since they can affect strongly the output signal, and hence impact on the control quality of the system. The PSO algorithm will be employed in this work to determine three scaling factors of the FL speed controller applied to an SRM drive. This means that each group of coefficients K_i (i = 1, 2, 3) expressed in (10) will be modified by using three updating factors α, β, and γ, respectively (see Fig. 3). Two new factors are able to be obtained as:

$$K'_P = \mu_2.(\beta.K_2).(\gamma.K_3) \tag{11}$$

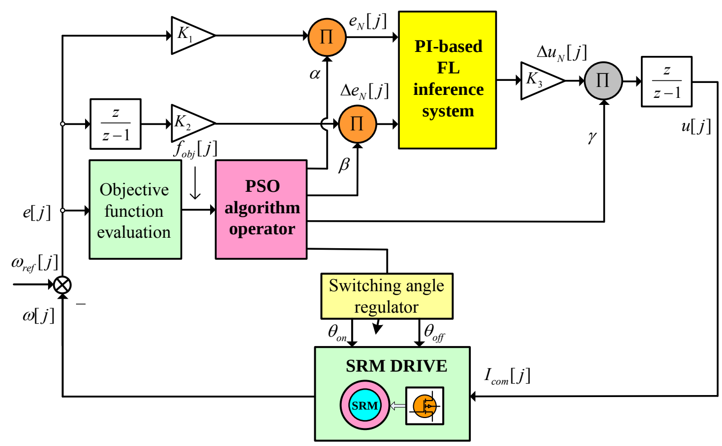

Fig. 3. Improved speed controller architecture based on PI-type FL for SRM

$$K'_I = \mu_1.(\alpha.K_1).(\gamma K_3). \tag{12}$$

According to the working mechanism of the PSO algorithm, the objective function is very important. Here, it can be defined depending upon the crucial aims of an effective speed controller. Obviously, such a speed regulator must be able to attain the minimum rise time and settling time as well as no overshoot. Thus, an objective function can be utilized as follows:

$$f_{obj} = \int_0^t t.e(t)dt = \int_0^t t.\left(\omega_{ref} - \omega(t)\right)dt. \tag{13}$$

It is clear that the above function f_{obj} needs to be minimized to meet an acceptable value, following the working mechanism of the PSO [12]. This function is executed inside the block named "Objective function evaluation" (see Fig. 3).

In this study, the PSO algorithm is applied to determine not only the scaling factors of the PI – type FLC but also two switching angles, namely, turn-ON angle θ_{ON} and turn-OFF angle θ_{OFF}. They are implemented inside a block named "Switching angle regulator" (see Fig. 3). It is the fact that such two switching angles impact significantly on the electromagnetic torque generation of the SRMs. The control performances of an SRM drive system will also be affected as a result, leading to the need of optimizing such two factors.

In this study, θ_{ON} and θ_{OFF} can also be optimized by using the PSO method. To perform it, two arguments need to be added to the variable space of the PSO algorithm. Hence, there are totally five variables used in such PSO method, including three for gain updating factors (α, β, γ) and two for switching angles (θ_{ON} and θ_{OFF}). Using the trial and error method, the lower and upper bounds of the turn-ON angle and the turn-OFF angle applied in the case study of a three-phase SRM drive can be determined respectively as follows:

$$28° \leq \theta_{ON} \leq 48° \tag{14}$$

$$67° \leq \theta_{OFF} \leq 88° \tag{15}$$

The optimization process based on the PSO algorithm will be carried out as mentioned earlier. Accordingly, the optimal control strategy proposed will be represented finally in Fig. 3. The effectiveness and feasibility of the proposed control strategy will be discussed in the following section.

5. Numerical Simulation

In this section, numerical simulation processes using MATLAB/Simulink package will be implemented to verify the superiority and feasibility of the proposed control architecture. The simulation diagram built in Simulink environment is dependent upon Fig. 3 for a typical three-phase SRM (6/4-type machine). In this work, to validate the outstanding performances of the proposed FL-based speed control strategy, a conventional speed regulator using PI will also be utilized. On the other hand, to simplify the control implementation, the PI-type current controllers are employed for the SRM drive. The PSO algorithm, which is executed by an *m*-file written in MATLAB/Script environment, will be applied to design the adaptive control methodology as mentioned earlier. Based on the implementation of the PSO method, two simulation cases are considered as:

(i) Case 1: The PSO algorithm is only applied to optimize three updating factors in order to design an adaptive PSO-PI-type FL speed controller. In this case, two switching angles are determined by using the trial and error method. In addition, a load torque condition (T_L = 100 *N.m*) is taken to the SRM drive at 0.6*s* to evaluate the dynamic behavior of the control system using different controllers.

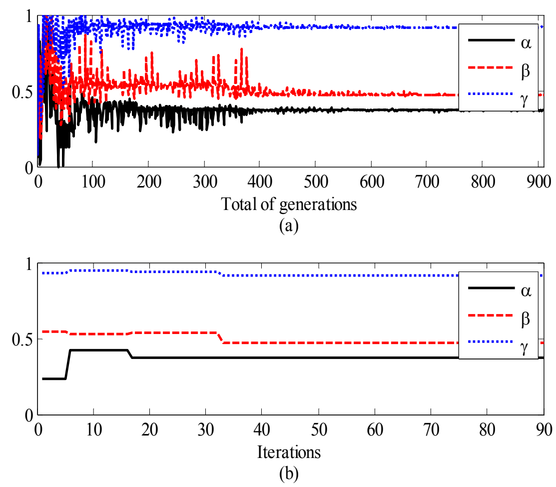

Fig. 4. Convergence of three updating factors in the first simulation case

(ii) Case 2: The PSO algorithm is used to determine not only three updating factors but also two switching angles. Hence, in this case, there are totally five variables need to be optimized in order to design the adaptive control methodology for the SRM drive. A complex-practical load torque, which will be mentioned below, is applied to this case to obtain an effective comparison between two control strategies: using the conventional PI speed regulator and the adaptive PSO-PI-type FL speed controller.

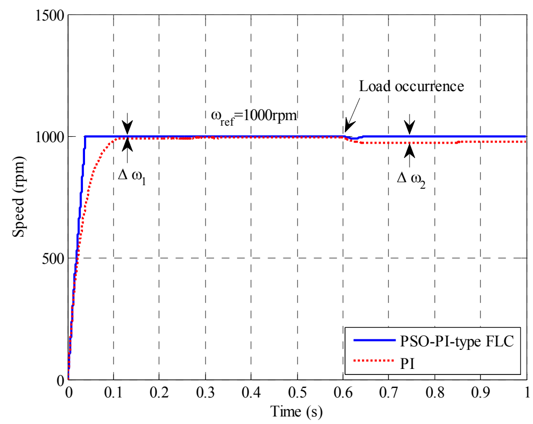

Fig. 5: Speed response for the first simulation case

Simulation parameters are given in the Appendices of the present paper. The simulation results for the first case are described in Figs. 4-5. Meanwhile, Figs. 6-7 show the results for the second simulation case.

In the first simulation case, as shown in Fig. 4, the convergence representing the objective function value of the PSO method (with $N = 90$) can be obtained. Using three optimized factors (α, β and γ) resulting from the PSO mechanism together with two switching angles obtained by using the trial and error method (i.e., $\theta_{ON} = 44°$ and $\theta_{OFF} = 79°$), the dynamic responses of the angular speed for two controllers, PI and PSO-PI-type FL, can be achieved as plotted in Fig. 5. It is found clearly the proposed FL-based controller obtains the better control performances in comparison with that of the conventional PI regulator. The angular speed resulting from the proposed control methodology is able to reach the reference value ($\omega_{ref} = 1000rpm$) much faster. Furthermore, even when a load torque occurs (T_L = 100 $N.m$ at 0.6s), the dynamic response of the PSO-PI-type FL controller is still efficient enough to recover the constant value of the speed as rapidly as possible. In contrast, at that moment, the angular speed resulting from the conventional PI regulator is fallen and may not be able to recover the constant reference value within a small period (see Fig. 5). Two speed deviations before and after the load torque appearance (i.e., $\Delta\omega_1$ and $\Delta\omega_2$) reveal the outstanding performances of the proposed control scheme for the SRM drive.

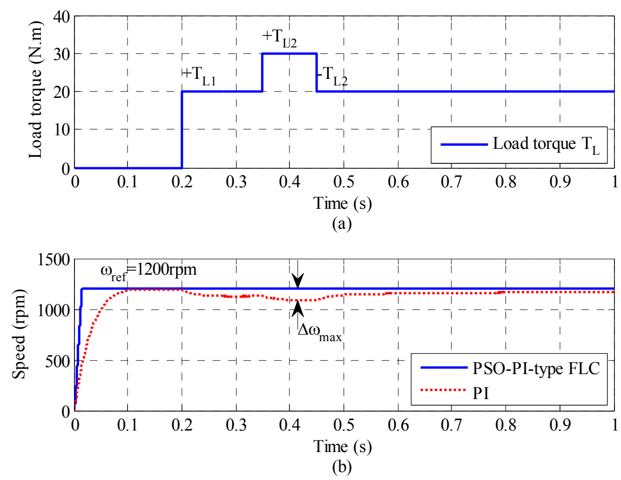

Fig. 6. Load and speed response in the second case
(a) Load torque; (b) Dynamic response of the speed

In the second simulation case, a complicated-practical load torque, shown in Fig. 6(a), is embedded in the drive system. With the enough number of iterations (N = 100), the value of the convergent objective function is much smaller than that of the first case, revealing the controller applying the PSO algorithm in this case can obtain the better control quality. Specifically, Fig. 6(b) shows the transient speed resulting from the two controllers considered in this paper. Similar to the first case, when treating a reference speed (ω_{ref} = 1200*rpm*), the proposed FL control architecture can achieve the steady state much more quickly than the conventional PI-based scheme. In addition, there is no reduction of the speed due to the load occurrence when applying the PSO-PI-type FL speed controller. This is obviously impossible to be obtained when using the PI speed regulator. Here, the maximum speed reduction resulting from such a PI regulator can be calculated as follows:

$$\Delta\omega_{\max} = \max_{t_0 \le t \le t_{\max}} \left(\omega_{ref} - \omega(t)\right) \tag{16}$$

where t_0 is the time at which the load torque is embedded and t_{max} is the maximum simulation time. Using (16), the maximum speed reduction in this case is greater than 110 *rpm*, representing approximately 10% of the reference value. This leads to the drawback of the conventional PI regulator when applied to control the speed of an SRM drive system. On the other hand, this further demonstrates the superiority of the proposed PSO-based FL controller when maintaining the angular speed of the machine. Fig. 7 describes the dynamic response of motor torque resulting from these two speed controllers. It is clear from Fig. 7 that the starting and working torques of the SRM drive system in terms of using the proposed FLC is larger than that of the PI regulator, leading to the superiority of the robust speed FLC introduced in this study.

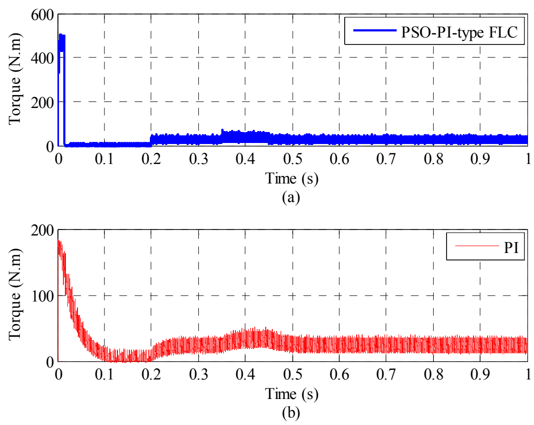

Fig. 7. Dynamic response of moment in the second case
(a) For PSO-PI-type FLC; (b) For the conventional PI controller

6. Conclusions

An adaptive PSO-based PI-type FL speed control strategy for the SRM drive system has been investigated in this paper. In principle, the PSO algorithm is applied to tune three scaling factors of the PI-type FL reasoning system as well as two switching angles of an SRM, which can affect strongly the control performances of the drive system. Numerical simulation results for a typical three phase SRM drive applying two types of the speed controllers (i.e., conventional PI and adaptive PSO-PI-based FL regulator) with various cases of the load torques have demonstrated the feasibility and effectiveness of the proposed control methodology. The dynamic responses of the angular speed resulting from the adaptive FL controller are much better than those of the conventional PI regulator. Along with the large starting and running torques obtained, the SRM drive system applying the proposed control architecture would be able to become a promising candidate when designing an effective traction control system. It is actually the main contribution of this study.

REFERENCES

1. *M. Balaji, V. Kamaraj*, "Evolutionary computation based multi-objective pole shape optimization of switched reluctance machine", Electr. Power Energy Syst., vol. 43, no. 1, 2012, pp. 63-69.

2. *M. Ahmad*, High Performance AC Drives Modeling Analysis and Control, Springer, London, UK, 2010.
3. *H. Wang*, *J. Liu*, *J. Bao*, *B. Xue*, "A novel bearingless switched reluctance motor with a biased permanent magnet", IEEE Trans. Ind. Electron., vol. 61, no. 12, 2014, pp. 6947-6955.
4. *P. Andrada*, *B. Blanque*, *E. Martinez*, *M. Torrent*, "A novel type of hybrid reluctance motor drive", IEEE Trans. Ind. Electron., vol. 61, no. 8, 2014, pp. 4337-4345.
5. *D.H. Lee*, *Z.G. Lee*, *J. Liang*, *J.W. Ahn*, "Single-phase SRM drive with torque Ripple reduction and power factor correction", IEEE Trans. Ind. Appl., vol. 43, no. 6, 2007, pp.1578-1587.
6. *R. Madhavan*, *B.G. Fernandes*, "Performance improvement in the axial flux-segmented rotor-switched reluctance motor", IEEE Trans. Energy Conver., vol. 29, no. 3, 2014, pp. 641-651.
7. *J. Cai*, *Z. Deng*, *R. Hu*, "Position signal faults diagnosis and control for switched reluctance motor", IEEE Trans. Magn., vol. 50, no. 9, 2014, pp. 1-11.
8. *L. Jihong*, "On methods for improving performance of PI-type fuzzy logic controllers", IEEE Trans. Fuzzy Syst., vol. 1, no. 4, 1993, pp. 298-301.
9. *K.B. Bimal*, Modern power electronics and AC drives, Prentice Hall PTR, Upper Saddle River, NJ, USA, 2002.
10. *R.K. Mudi*, *N.R. Pal*, "A robust self-tuning scheme for PI- and PD-type fuzzy controllers", IEEE Trans. Fuzzy Syst., vol. 7, no. 1, 1999, pp. 2-16.
11. *S. Mir*, *M.S. Islam*, *T. Sebastian*, *I. Husain*, "Fault-tolerant switched reluctance motor drive using adaptive fuzzy logic controller", IEEE Trans. Power Electr., vol. 19, no. 2, 2004, pp. 289-295.
12. *D.V. Yamille*, *K.V. Ganesh*, *M. Salman*, *H. Jean-Carlos*, *G.H. Ronald*, "Particle swarm optimization: basic concepts, variants and applications in power systems", IEEE Trans. Evol. Comput., vol. 12, no. 2, 2008, pp. 171-195.

APPENDICES

A1. Parameters for the three-phase 6/4 SRM model

$$R_k = 0.05\Omega, J = 0.05kg.m^2, f = 0.02N.m.s, L_k^{\min} = 0.67mH, L_k^{\max} = 23.6mH, i_k^{\max} = 500A$$

A2. Parameters for implementing the PSO algorithm

The first simulation case: $n = 3,\ m = 10,\ N = 90,\ \overrightarrow{Lb} = [0,0,0], \overrightarrow{Ub} = [1,1,1]$

The second simulation case:

$$n = 5, m = 10, N = 100; \overrightarrow{Lb} = [0,0,0,28,67]; \overrightarrow{Ub} = [1,1,1,48,88]$$

A3. Simulated parameters for the PI-like FLC inference system

Initial parameters: $K_1 = K_2 = K_3 = 0.5$